Research Paper

Brain and Neuroscience Advances

Brain and Neuroscience Advances
Volume 2: 1–13

DOI: 10.1177/2398212818794820
journals.sagepub.com/home/bna
SAGE

Hyperglycaemia does not increase perfusion deficits after focal cerebral ischaemia in male Wistar rats

Lisa A. Thow, Kathleen MacDonald, William M. Holmes, Keith W. Muir, I. Mhairi Macrae and Deborah Dewar

Abstract

Background: Hyperglycaemia is associated with a worse outcome in acute ischaemic stroke patients; yet the pathophysiological mechanisms of hyperglycaemia-induced damage are poorly understood. We hypothesised that hyperglycaemia at the time of stroke onset exacerbates ischaemic brain damage by increasing the severity of the blood flow deficit.

Methods: Adult, male Wistar rats were randomly assigned to receive vehicle or glucose solutions prior to permanent middle cerebral artery occlusion. Cerebral blood flow was assessed semi-quantitatively either 1 h after middle cerebral artery occlusion using ^{99m}Tc-D, L-hexamethylpropyleneamine oxime (^{99m}Tc-HMPAO) autoradiography or, in a separate study, using quantitative pseudo-continuous arterial spin labelling for 4 h after middle cerebral artery occlusion. Diffusion weighted imaging was performed alongside pseudo-continuous arterial spin labelling and acute lesion volumes calculated from apparent diffusion coefficient maps. Infarct volume was measured at 24 h using rapid acquisition with refocused echoes T_2-weighted magnetic resonance imaging.

Results: Glucose administration had no effect on the severity of ischaemia when assessed by either ^{99m}Tc-HMPAO autoradiography or pseudo-continuous arterial spin labelling perfusion imaging. In comparison to the vehicle group, apparent diffusion coefficient–derived lesion volume 2–4 h post-middle cerebral artery occlusion and infarct volume 24 h post-middle cerebral artery occlusion were significantly greater in the glucose group.

Conclusions: Hyperglycaemia increased acute lesion and infarct volumes but there was no evidence that the acute blood flow deficit was exacerbated. The data reinforce the conclusion that the detrimental effects of hyperglycaemia are rapid, and that treatment of post-stroke hyperglycaemia in the acute period is essential but the mechanisms of hyperglycaemia-induced harm remain unclear.

Keywords

Cerebral blood flow, animal model, hyperglycaemia, magnetic resonance imaging, focal ischaemia

Received: 2 March 2018; accepted: 12 July 2018

Introduction

Hyperglycaemia occurs in over 60% of stroke patients with no previous history of diabetes and in 90% of diabetics (Muir et al., 2011). Post-stroke hyperglycaemia (PSH) is associated with increased mortality, poor functional outcomes and larger final infarct sizes (Bevers et al., 2016; Melamed, 1976; Shimoyama et al., 2016). The association between hyperglycaemia and unfavourable prognosis is particularly evident in ischaemic stroke patients without a known history of diabetes mellitus (Capes et al., 2001; Shimoyama et al., 2014). Glucose-lowering treatment for PSH carries a risk of hypoglycaemia (Gray et al., 2007; McCormick et al., 2010; Staszewski et al., 2011), raising safety concerns over this type of intervention. Therefore, elucidation of the pathophysiological mechanisms that lead to the detrimental effects of PSH may present alternative therapeutic avenues. We previously reported that hyperglycaemia in rats, *at levels typically experienced by stroke patients*, exerted detrimental effects on ischaemic brain tissue in the very acute period following induction of focal cerebral ischaemia (Tarr et al., 2013). Using diffusion-weighted magnetic resonance imaging (MRI) to define the temporal evolution of tissue damage, as defined by the apparent diffusion coefficient (ADC), larger ADC-defined lesions were observed in hyperglycaemic compared to normoglycaemic rats as early as 1 h after middle cerebral artery occlusion (MCAO). These data indicate that hyperglycaemia adversely affects the ischaemic brain in the very acute period after arterial occlusion.

Given the very early nature of the detrimental influence of PSH, one of the potential mechanisms is an effect on cerebral perfusion. If hyperglycaemia reduces cerebral blood flow (CBF), this could increase the severity of the ischaemic insult leading to

Institute of Neuroscience & Psychology, College of Medical, Veterinary & Life Sciences, University of Glasgow, Glasgow, UK

Corresponding author:
Deborah Dewar, Institute of Neuroscience & Psychology, College of Medical, Veterinary & Life Sciences, University of Glasgow, Garscube Estate, Glasgow G61 1QH, UK.
Email: Deborah.Dewar@glasgow.ac.uk

a larger perfusion deficit and potentially more brain tissue damage. There is some evidence from preclinical studies that hyperglycaemia can reduce CBF in both non-ischaemic rat brain (Duckrow et al., 1985, 1987), and after induction of focal cerebral ischaemia in rats (Kawai et al., 1998), and cats (Wagner et al., 1992). Several mechanisms for hyperglycaemia-induced reductions in CBF have been proposed from these preclinical studies including turbulent cerebral capillary blood flow resulting in damage to the endothelium (Huang et al., 2014), altered osmolality and increased cerebral vascular resistance (Duckrow, 1995), impairment of nitric oxide-dependent dilatation of cerebral arterioles via the activation of protein kinase C (Mayhan and Patel, 1995) and a co-operative effect of hyperglycaemia and cortical spreading depression on CBF (Wang et al., 2008). However, limitations of previous animal studies include the use of either type I diabetes models or induction of blood glucose levels that are much higher than what is observed in acute stroke patients (MacDougall and Muir, 2011). We therefore sought to determine whether clinically relevant hyperglycaemia increases the severity of cerebral ischaemia and causes greater ischaemic damage in the acute period following induction of focal cerebral ischaemia in rats. We used two distinct techniques for assessing CBF in separate experiments: ^{99m}Tc-D, L-hexamethylpropyleneamine oxime (^{99m}Tc-HMPAO) blood flow autoradiography which provides high spatial and anatomical resolution at a single time point and pseudo-continuous arterial spin labelling (pCASL) for repeated measurements of CBF in the same animal over time. Diffusion weighted imaging (DWI) was performed alongside pCASL to measure ADC lesion volume in order to calculate the volume of perfusion–diffusion (PI-DWI) mismatch tissue during the first 4 h after MCAO. PI-DWI mismatch tissue is widely used to identify the ischaemic penumbra and MRI studies in acute ischaemic stroke patients show that larger infarcts in patients with admission hyperglycaemia are associated with reduced penumbral salvage (Parsons et al., 2002; Rosso et al., 2011). The suggestion that PI-DWI mismatch tissue might be highly susceptible to hyperglycaemia through the accelerated conversion of hypoperfused at-risk tissue to infarction provided a rationale for comparing the volume of PI-DWI mismatch tissue in glucose- and vehicle-injected animals. The issue of when hyperglycaemia occurs in stroke patients is very hard to define since in most cases hyperglycaemia is present on hospital arrival 3–6 h after symptom onset, but in most of these cases it predates the stroke as it reflects underlying disordered glycaemic control. A smaller group then develops hyperglycaemia at some stage of their initial 48 h hospital stay, but it is the first group with 'admission hyperglycaemia' that is of clinical interest as this is the group for whom the outcome after stroke is poor (Muir et al., 2011). The current study was not designed to mimic the time course of hyperglycaemia in stroke patients which is heterogeneous, but rather to test the mechanistic hypothesis that clinically relevant levels of hyperglycaemia *at the time of MCAO* would increase the perfusion deficit.

Materials and methods

Animals

Experiments were carried out under licence from the UK Home Office and were subject to the Animals (Scientific Procedures) Act, 1986. All experiments were performed in compliance with the ARRIVE (Animal Research; Reporting In Vivo Experiments) guidelines. Adult, male Wistar rats (Harlan, UK) weighing between 280 and 370 g were used in all experiments and prior to surgery were housed in standard cages in groups of 2–4. In recovery experiments, rats were singly housed after recovery until termination. All rats were randomised to receive a vehicle or glucose injection using an online randomisation plan generator (www.randomization.com). The vehicle and glucose solutions for injection were prepared by technical staff and therefore, the investigators who performed surgery, autoradiography, MRI scanning and analyses were blinded to the treatment group identity throughout. Investigators (L.T., K.M.) who performed the autoradiographic and MRI analyses were unblinded to rat identity only after data analyses had been scrutinised and finalised by other authors.The investigators who performed surgery also recorded blood glucose levels and were therefore not blinded to the glucose level results during the procedure. Rats were fasted overnight (in pairs) prior to surgery with free access to water.

MCAO surgery and glucose administration

Surgeries were performed first thing in the morning. Animals were intubated and artificially ventilated under isoflurane anaesthesia (5% induction, 2.5% maintenance in 70% N_2O/30% O_2). The right femoral artery was cannulated for continuous recording of mean arterial blood pressure (MABP) and monitoring of blood pH, $PaCO_2$, PaO_2 and blood glucose. The femoral vein was cannulated in some animals for intravenous administration of ^{99m}Tc-HMPAO. Permanent focal cerebral ischaemia was achieved by occluding the distal portion of the middle cerebral artery (MCA) using diathermy, a modification of the method described by Tamura and colleagues (Tamura et al., 1981). The left MCA was exposed via a craniectomy and the point at which the MCA crosses the inferior cerebral vein was identified and a ~1 mm length of the artery above and below this point was electrocoagulated with diathermy forceps. The MCA was then cut with microscissors to confirm complete occlusion.

Ten minutes prior to MCAO animals received a single intraperitoneal injection (10 mL/kg) of either a 15% glucose solution in distilled water or vehicle solution. We have previously demonstrated that with this protocol, blood glucose rises to hyperglycaemic levels within 1 h (Tarr et al., 2013). Arterial blood glucose levels were measured 20 min before MCAO to obtain a baseline reading and at selected time points after MCAO using a glucometer (Accu-Chek, Roche, Germany).

CBF measurement using ^{99m}Tc-HMPAO autoradiography

At 1 h post-MCAO 225MBq of ^{99m}Tc-HMPAO in 0.6 mL saline was injected intravenously over 30 s. Five minutes following injection, rats were euthanised by decapitation and brains were removed, frozen in isopentane (−45°C) and 20 µm sections cut on a cryostat. Sections spanning the entire cerebrum were mounted onto glass slides and autoradiograms were prepared from these sections by exposing them, alongside pre-calibrated ^{14}C standards ($21-174\times10^3$ nCi/g ^{99m}Tc tissue equivalents), for 1 h. The ^{99m}Tc tissue concentrations on the autoradiograms were analysed using an image analysis system (MCID; Imaging Research,

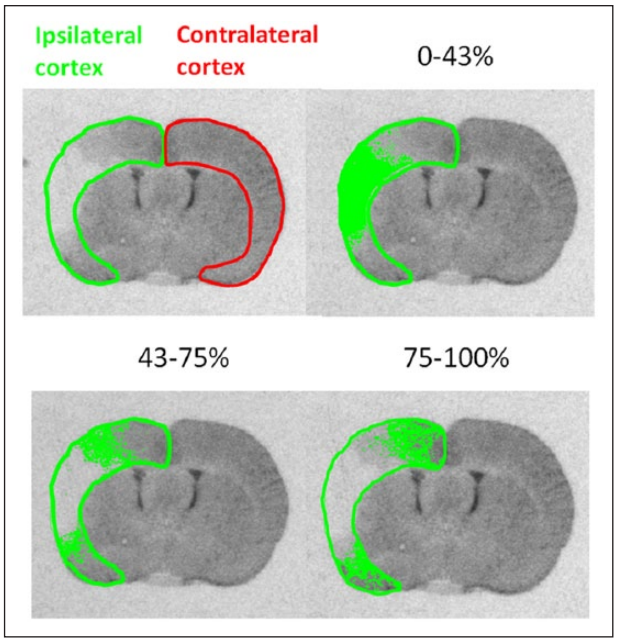

Figure 1. Representative autoradiograms depicting threshold analysis of ^{99m}Tc-HMPAO uptake. The cortex ipsilateral to MCAO (outlined in green) and contralateral cortex (outlined in red) was manually delineated (top left). The pale region in the ipsilateral cortex represents an area with reduced uptake of ^{99m}Tc-HMPAO indicating reduced CBF induced by MCAO in the cerebral cortex. In subsequent images, the green pixels represent the area of the ipsilateral cortex where ^{99m}Tc-HMPAO uptake was within 0%–43%, 43%–75% and 75%–100% of the contralateral cortex.

Linton, Cambridge, UK) and were considered to be proportional to CBF. CBF was assessed using two different analyses: threshold and region of interest (ROI).

Threshold analysis

CBF in the cortex ipsilateral to the occluded MCA was normalised to the contralateral cortex to minimise the influence of inter-animal variability. To assess the severity of the CBF deficit 1 h post-MCAO, a threshold approach to the analysis of the autoradiograms was taken. CBF in the ischaemic cortex was examined using three thresholds: 0%–43%, 43%–75% and 75%–100% of the non-ischaemic cortex. The 0%–43% range was selected to represent severely hypoperfused or ischaemic core tissue. This has previously been shown to be a viability threshold identifying irreversibly damaged tissue after MCAO in rats using MRI (Shen et al., 2003). The 43%–75% and 75%–100% thresholds were selected to represent moderately and mildly hypoperfused tissue, respectively. For each animal, autoradiographic images of 10 coronal levels (ranging 4.7 mm anterior to Bregma and 8 mm posterior to Bregma) were captured for threshold analysis. The area of the ipsilateral cortex at each threshold was measured and expressed as a percentage of the area of the ipsilateral cortex. For each coronal level, CBF was measured on three consecutive sections and the average was calculated. Representative autoradiograms depicting threshold analysis at coronal level 3 (0.3 mm posterior to Bregma) are shown in Figure 1.

ROI analysis

A total of 22 distinct brain structures were selected for ROI analysis and a rat brain atlas (Paxinos, 2007) was used to identify each structure in the autoradiograms. Autoradiographic images depicting the uptake of ^{99m}Tc-HMPAO within selected brain sections were captured for ROI analysis. The rectangle drawing tool on the image analysis system was used to place a box over each structure in the ipsilateral hemisphere and the optical density measured. ^{99m}Tc-HMPAO tissue concentration (nCi/g) was then calculated with reference to the optical densities of the standards. The same tool was used to place an identical sized box over the equivalent ROI in the contralateral hemisphere to calculate the concentration there. The ^{99m}Tc-HMPAO tissue concentration from the ROI in the ipsilateral hemisphere was then expressed as a percentage of that in the contralateral hemisphere. For each ROI examined, the ^{99m}Tc-HMPAO concentration was determined in three autoradiographic sections and the average was taken.

CBF measurement using MRI perfusion imaging

MRI data were acquired using a Bruker Biospec 7T/30 cm system with a gradient coil (internal diameter = 121 mm, 400 mT/m) and a 72 mm birdcage resonator. Following surgery to induce MCAO rats was immediately transferred to a Perspex rat cradle and the head was restrained using tooth and ear bars. A linear phased array surface receiver coil (2 cm diameter) was placed above the head of the animal. Body temperature was monitored using a rectal thermocouple and maintained within physiological range (37°C ± 0.5°C) using a temperature-controlled water jacket. MABP was monitored via the femoral artery catheter attached to a blood pressure transducer, which was in turn connected to a computer in combination with an MP150 Biopac System (Biopac Systems Inc, USA) and Acknowledge software (Linton). MRI scanning was performed each hour post-MCAO for a total of 4 h. During each hour, quantitative imaging of CBF was carried out on six coronal slices within the MCA territory using a form of pCASL. The sequence employs a Spin-Echo Echo Planar Imaging (SE-EPI) module (echo time = 20 ms, repetition time = 7000 ms, matrix = 96 × 96, field of view (FOV) = 25 × 25 mm^2, slice thickness 1.5 mm, 16 averages, 4 shots) preceded by 50 hyperbolic secant inversion pulses in a 3 s train (Baskerville et al.). A T_1-weighted image was also acquired each hour using an EPI inversion recovery sequence (echo time = 20 ms, repetition time = 10,000 ms, matrix = 96 × 96, FOV = 25 × 25 mm, slice thickness 1.5 mm, 16 averages, 4 shots, using 16 inversion times from 200 to 7700 ms).

Quantitative CBF maps (units: mL/100 g/min) were calculated using the formula for continuous labelling (Williams et al., 1992), which has been described elsewhere (Baskerville et al., 2012; Reid et al., 2012). ImageJ software was used to process raw data sets.) Labelled pCASL images were generated when blood was excited by a radiofrequency pulse (RF) at the level of the carotid arteries in the neck to produce an endogenous ‘label’. These were subtracted from control images (no RF pulse) and then divided by control images to generate relative CBF maps. Quantitative CBF maps were generated by dividing the relative CBF map by the T_1 values generated from the T_1 map. Perfusion deficit maps were produced by applying a previously published

abnormal perfusion threshold of 30 mL/100 g/min (Shen et al., 2003) to all pCASL images (see explanation below).

DWI

Following MCAO, DWI reveals evidence of ischaemic injury to brain tissue within minutes of the arterial occlusion and can be used serially over the acute stroke period (0–4 h) to track changes in lesion size. DWI was therefore also performed each hour in order to map the evolution of the ischaemic lesion (SP-EPI, echo-time = 22.5 ms; repetition time = 4 s, in-plane resolution of 260 µm; three directions: x, y, z; B values: 0, 1000 s/mm^2, eight slices 1.5 mm thickness). Quantitative ADC maps (mm^2/s) were calculated from the DWI scans using ParaVision v5 (Bruker, Germany) and subsequently analysed using ImageJ software. On all ADC maps, the ADC lesion volume was calculated using a previously published threshold of 0.53×10^{-3} mm^2/s (Shen et al., 2003).

There is currently no consensus on where to set the perfusion and diffusion thresholds to accurately define perfusion and diffusion lesions in rodent models of focal cerebral ischaemia (Campbell and Macrae, 2015). To generate ADC and CBF thresholds, Shen et al. (2003) adjusted the ADC and CBF values on respective ADC and CBF maps until the ADC- and CBF-defined lesion volumes were numerically equal to infarct volumes measured at 24 h post-MCAO. The absolute ADC and CBF thresholds established in the study by Shen et al. (2003) were 0.53×10^{-3} mm^2/s and 30 mL/100 g/min, respectively, and thus, they were applied in the current study.

T_2-weighted imaging

The time course of T_2 signal change reflects net tissue water content and this changes slowly over the early hours of ischaemia (Hoehn-Berlage et al., 1995). However, by 24 h, T_2 imaging delineates the extent of the ischaemic lesion and is the most regularly used MRI sequence to determine the extent of the infarct. Animals were recovered from anaesthesia after pCASL and DWI MRI scanning for 24 h at which time they were re-anaesthetised (5% isoflurane in 70/30 N_2O/O_2 mixture) and transferred to the MRI scanner where anaesthesia was maintained via a facemask (2.5% isoflurane 70/30 N_2O/O_2 mixture). A RARE (rapid acquisition with refocused echoes) T_2-weighted sequence (effective TE: 46.8 ms, TR: 5000 s; in-plane resolution of 97 µm; 16 slices of 0.75 mm thickness) was used to determine infarct volume at 24 h post-MCAO. The infarct was defined as the hyperintense area on T_2-weighted images. ImageJ was used to measure the area of the hyperintense region on each of the 16 slices and infarct volume was calculated by summing the total area across the 16 slices and multiplying by the slice thickness. The volumes of the ipsilateral and contralateral hemispheres were also determined. All infarct volume calculations were corrected for oedema using published equations (Gerriets et al., 2004; Swanson et al., 1990).

Calculation of the penumbra from the perfusion–diffusion mismatch

A spatial assessment of the perfusion–diffusion mismatch was carried out on each of the six coronal slices of the CBF maps. The mismatch was defined using previously published ADC (0.53×10^{-3} mm^2/s) and CBF (30 mL/100 g/min) thresholds (Shen et al., 2003). The area of mismatch on each of the six slices was measured, summed and multiplied by the slice thickness (1.5 mm) to obtain the volume of mismatch tissue. This was repeated for each time point after MCAO.

Western blot analysis

Brains were available from all animals that completed the MRI scanning and therefore as an observational analysis (not part of the formal study), these were analysed by Western blotting to examine proteins that are associated with ischaemic brain damage (membrane-associated spectrin and microtubule-associated protein 2). Following the T_2 scan at 24 h after MCAO, the ipsilateral ischaemic cortex was dissected and homogenised in lysis buffer (250 mM sucrose, 10 mM Hepes, 1 mM sodium orthovanadate, 1 mM sodium pyrophosphate, 1 mM ethylenediaminetetraacetic acid (EDTA) 0.2 mM phenylmethylsulfonyl fluoride) supplemented with a protease inhibitor cocktail (Sigma, UK). Lysates were then separated into a crude membrane fraction by centrifugation. The protein concentrations of the samples from the membrane fraction were determined using a bicinchoninic acid (BCA) protein assay kit (Fisher Scientific, UK). 10 g of protein from the membrane fraction of each animal was electrophoresed on 4%–20% Criterion™ TGX pre-cast gels (Bio-Rad, UK) and transferred to a nitrocellulose membrane. The membrane was blocked with 5% milk powder in 1× Tris-buffered saline containing 1% Tween-20 (in Tris-buffered saline) to minimise non-specific binding for 1 h then incubated overnight at 4°C with the following primary antibodies: monoclonal mouse anti-spectrin (MAB1622, Millipore, UK), polyclonal rabbit anti-MAP2 (ab32454, Abcam, UK), both diluted at 1:200,000, and monoclonal mouse anti-beta-Actin (ab8224, Abcam, UK) (diluted at 1:400,000). The membrane was incubated with the secondary antibody (1:10,000, Dako) and Bio-Rad's Clarity Western enhanced chemi-luminescence (ECL) substrate was used according to the manufacturer's protocol. Membranes were visualised using the Bio-Rad Chemidoc MP system and ImageJ software was used to estimate the amount of protein in each sample.

Sample size calculation

A sample size calculation was performed based on an 80% power ($1-\beta = 0.8$) and a 95% significance level ($\alpha = 0.05$). The effect size (50 mm^3) and standard deviation (36.5) were determined from a previous in-house study (Tarr et al., 2013) and were based on the change in ADC-derived lesion volume at 1 h post-MCAO exhibited in hyperglycaemic compared to normoglycaemic WKY rats. The number of animals per group was calculated to be 9.

Inclusion/exclusion criteria

A total of 26 animals were entered into the autoradiography study and 5 were excluded (2 glucose-treated rats and 3 vehicle-treated rats). Three of the five rats died due to significant blood loss during the diathermy step of MCAO. One of the rats died during the

injection of ^{99m}Tc-HMPAO and one rat was excluded from analysis due to the presence of a haemorrhage in the brain which was detected as it was being sectioned. The final group sizes for the autoradiography study were n = 10 for the vehicle treatment group and n = 11 for the glucose treatment group. A total of 27 animals were entered into the MRI study and 4 were excluded (3 vehicle-treated rats and 1 glucose-treated rat) as they died during or after the MRI scanning protocol. Three further rats (all glucose treated) were excluded from the study due to the presence of subdural haematomas on T_2-weighted images. The final group sizes for the MRI study analysis were n = 10 for the vehicle treatment group and n = 10 for the glucose treatment group.

Table 1. Physiological variables for the ^{99m}Tc-HMPAO blood flow study.

Physiological parameter	Vehicle (n = 10)	Glucose (n = 11)
Body weight (g)	313 ± 2	322 ± 3
MABP (mmHg)	85 ± 4	90 ± 4
$PaCO_2$ (mmHg)	39 ± 6	40 ± 4
PaO_2 (mmHg)	125 ± 1	120 ± 2
pH	7.4 ± 0.1	7.4 ± 0.1
Temperature (°C)	37 ± 0.2	37 ± 0.2
Blood glucose (mmol/L) at baseline	7.3 ± 1.3	7.1 ± 1.6
Blood glucose (mmol/L) 1 h post-MCAO	6.8 ± 0.8	11.9 ± 2.6***

Body weight was measured on the day of MCAO. MABP, body temperature, pH, PaO_2 and $PaCO_2$ were measured approximately every 30 min during surgery and the data are expressed as the mean ± standard deviation over the entire surgical period. Blood glucose was measured 20 min before MCAO and 1 h post-MCAO. All statistical comparisons by Student's unpaired t-test.
***$P < 0.0001$ compared with vehicle.

Statistical analysis

Physiological variables, CBF ROI measurements, T_2-derived infarct volumes and relative protein levels were analysed using an unpaired Student's t-test. Line graphs of the threshold analysis data were analysed using a two-way analysis of variance (ANOVA). ADC lesion volumes, perfusion deficit volumes and perfusion–diffusion mismatch were assessed using a repeated measures two-way analysis of variance (RM two-way ANOVA) with Bonferroni's post-test. A Pearson's correlation was used to measure the linear correlation between T_2-derived infarct volume at 24 h post-MCAO and blood glucose levels at 4 h post-MCAO. Differences between groups were considered to be statistically significant when $P < 0.05$. Data are expressed as mean ± standard deviation or presented as scatterplots with the mean indicated. Where images are presented from the median animal of each group, these are the median animals from the T_2-derived infarct volume results.

Results

Physiological variables

Physiological variables in animals from both autoradiography and MRI studies were within normal limits and there were no significant differences in body weight, MABP, body temperature, blood gases and pH between the vehicle and glucose groups (Tables 1 and 2). In both autoradiography and MRI studies, blood glucose levels were measured 20 min prior to MCAO to obtain a baseline reading. Mean blood glucose levels at baseline ranged from 4.9 to 7.3 mmol/L and were comparable between groups in each study (Tables 1 and 2). Following glucose or vehicle administration, blood glucose levels increased significantly in animals that received glucose compared to those that received the vehicle,

Table 2. Physiological variables for MRI the study.

Physiological parameter	Time post-MCAO Baseline	1h	2h	3h	4h
Vehicle (n = 10)					
Body weight (g)	321 ± 25				
MABP (mmHg)	92 ± 9	91 ± 10	90 ± 10	90 ± 8	89 ± 6
$PaCO_2$ (mmHg)	35 ± 10	36 ± 10	41 ± 11	41 ± 11	39 ± 5
PaO_2 (mmHg)	126 ± 2	125 ± 2	121 ± 2	131 ± 3	123 ± 3
pH	7.41 ± 0.1	7.38 ± 0.04	7.39 ± 0.04	7.40 ± 0.03	7.35 ± 0.04
Temperature (°C)	37 ± 0.3	37.4 ± 0.4	37.3 ± 0.5	37.3 ± 0.3	37.1 ± 0.1
Blood glucose (mmol/L)	4.9 ± 0.9	5.6 ± 1.5	6.5 ± 1.2	6.2 ± 0.8	6.1 ± 1.1
Glucose (n = 10)					
Body weight (g)	336 ± 17				
MABP (mmHg)	97 ± 10	88 ± 5	87 ± 11	85 ± 11	89 ± 7
$PaCO_2$ (mmHg)	37 ± 11	38 ± 6	37 ± 9	36.5 ± 5	41 ± 9
PaO_2 (mmHg)	132 ± 2	123 ± 2	122 ± 1	131 ± 2	132 ± 3
pH	7.47 ± 0.04	7.37 ± 0.1	7.35 ± 0.07	7.37 ± 0.1	7.37 ± 0.04
Temperature (°C)	37.0 ± 0.2	37.2 ± 0.4	37.1 ± 0.6	37.4 ± 0.4	37.2 ± 0.6
Blood glucose (mmol/L)	5.9 ± 1.1	11.3 ± 2.9****	11.2 ± 2.3****	11.1 ± 1.4****	10.8 ± 1.5****

Body weight was measured on the day of MCAO. MABP, $PaCO_2$, PaO_2, pH, temperature and blood glucose were measured at baseline (20 min before MCAO) and at each hour for 4 h after MCAO. The data are expressed as mean ± standard deviation. Statistical comparisons by Student's unpaired t-test or repeated measures two-way ANOVA with Bonferroni's post-test (blood glucose). ****$P < 0.0001$ compared with vehicle.

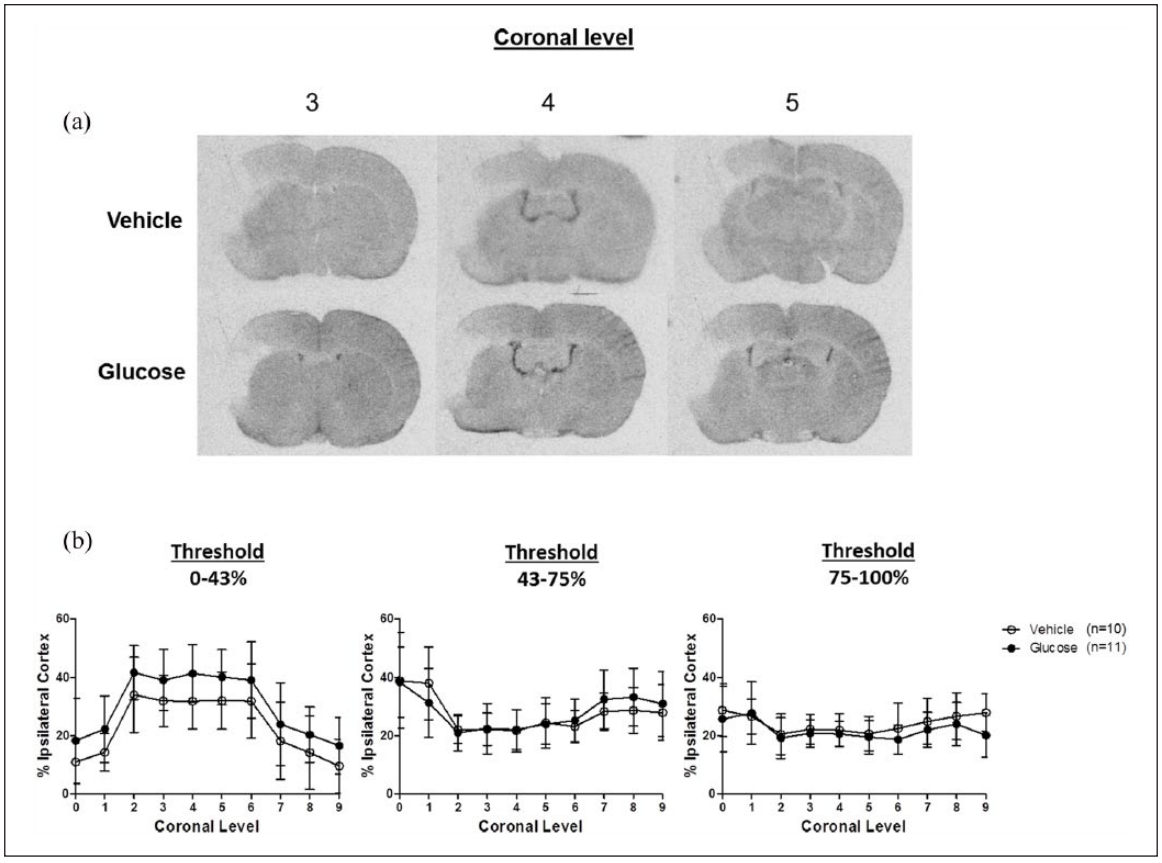

Figure 2. Autoradiograms showing ^{99m}Tc-HMPAO concentration in coronal levels 3, 4 and 5, at 1 h post-MCAO from a representative vehicle and glucose-treated rat (a). Ischaemia is visible topographically within the ipsilateral cortex in both groups to a similar extent. Line graphs illustrating the % area of the ipsilateral cortex, across 10 coronal levels (rostral to caudal), with CBF that is severely (0%–43%), moderately (43%–75%) and mildly (75%–100%) reduced relative to the contralateral cortex (b). Data are presented as mean ± standard deviation. Differences between groups are not statistically significant: two-way ANOVA.

in which blood glucose levels remained close to baseline levels. Blood glucose levels ranged from 10.8 to 11.9 mmol/L in animals that received glucose and from 5.6 to 6.8 mmol/L in animals that received vehicle (Tables 1 and 2).

^{99m}Tc-HMPAO autoradiography

We assessed CBF using autoradiography and MRI in two separate experiments. The results from the ^{99m}Tc-HMPAO experiments are presented in Figure 2. In all autoradiograms, regions of ischaemia were visible in the ipsilateral cortex where there was reduced uptake of the radiotracer ^{99m}Tc-HMPAO (Figure 2(a)). Autoradiograms were analysed using both a threshold and ROI-based analysis. For the threshold analysis, different thresholds were applied to the ipsilateral cortex of 10 coronal levels in order to grade the severity of ischaemia into three categories: severely (0%–43%), moderately (43%–75%) and mildly (75%–100%) reduced relative to the contralateral cortex. The area of the ipsilateral cortex at each threshold, at each coronal level, was measured and expressed as a percentage of the area of the ipsilateral cortex (Figure 2(b)). The differences between groups were not statistically significant at any of the thresholds examined. Using ROI analysis, we found that there were notable decreases in ^{99m}Tc-HMPAO uptake in ipsilateral, compared to contralateral brain structures supplied by the distal branches of the MCA in both the vehicle and glucose groups (Table 3). There were no statistically significant differences between the vehicle and glucose groups in any of the 22 structures examined (Table 3).

MRI perfusion imaging

The results from the MRI perfusion experiments are presented in Figure 3. Quantitative pCASL CBF maps acquired at 1 and 4 h post-MCAO from the median animal of each group are presented in Figure 3(a). Darker regions on the CBF maps represent regions of reduced CBF and the region of reduced blood flow induced by MCAO was detected in the ipsilateral cortex of all six coronal slices in both groups, at both time points. At each time point after MCAO, the mean volume of the perfusion deficit tended to be larger in the glucose group compared to the vehicle group (Figure 3(b)), but the difference between groups was not statistically significant. The volume of the perfusion deficit tended to increase over time in both groups. In the vehicle group, the mean perfusion deficit volume increased from $140 \pm 37\,mm^3$ at 1 h post-MCAO to $151 \pm 42\,mm^3$ at 4 h but the difference was not statistically significant. Similarly, in the glucose group, the mean

Table 3. Normalised ^{99m}Tc-HMPAO concentrations in 22 distinct brain regions following occlusion of the middle cerebral artery for 1 h.

Normalised ^{99m}Tc-HMPAO concentration (% of contralateral region)			
Region	Vehicle	Glucose	P value
Motor cortex	57 ± 18	60 ± 26	0.81
Auditory cortex	54 ± 28	53 ± 28	0.89
Visual cortex	50 ± 15	63 ± 23	0.43
Primary somatosensory cortex	18 ± 15	12 ± 5	0.22
Secondary somatosensory cortex	35 ± 19	25 ± 18	0.42
Anterior cingulate cortex	77 ± 16	81 ± 18	0.53
Medial cingulate cortex	96 ± 15	87 ± 21	0.29
Lateral orbital cortex	60 ± 28	62 ± 22	0.88
Insular cortex	68 ± 28	55 ± 19	0.21
Prelimbic cortex	78 ± 21	80 ± 18	0.80
Piriform cortex	89 ± 21	94 ± 19	0.56
Caudate putamen medial	95 ± 17	95 ± 9	0.87
Caudate putamen lateral	103 ± 20	98 ± 26	0.60
Hippocampus	106 ± 14	102 ± 5	0.31
Globus pallidus	112 ± 13	111 ± 11	0.85
Nucleus accumbens	99 ± 12	99 ± 10	0.92
Amygdala	105 ± 15	105 ± 12	0.95
Hypothalamus	99 ± 10	98 ± 5	0.88
Thalamus	103 ± 5	101 ± 7	0.40
Substantia nigra	105 ± 8	110 ± 11	0.20
Septum	98 ± 7	99 ± 6	0.56
Corpus callosum	100 ± 8	89 ± 10	0.40

Data are presented as means ± standard deviations (vehicle n=10; glucose n=11). Differences between groups are not statistically significant: Student's unpaired t-test.

perfusion deficit volume increased from 164 ± 40 to 192 ± 54 mm^3 between 1 and 4 h post-MCAO, respectively.

ADC lesion volume and T_2-derived infarct volume

The spatial profiles of the ADC lesions at 1 and 4 h post-MCAO from the median animal of each group are presented in Figure 4(a). In the glucose animal, the ADC lesion is anatomically more widespread than in the vehicle animal. At 1 h after MCAO, there was no significant difference in the mean ADC-defined lesion volume between the vehicle and glucose groups (Figure 4(b)). However, ADC lesion volumes measured at 2, 3 and 4 h after MCAO were significantly greater in the glucose group compared to the vehicle. T_2-derived infarct volume measured 24 h after MCAO was significantly greater in glucose compared to vehicle-treated rats (Figure 5(a). The mean T_2-derived infarct volume was 57 ± 22 and 90 ± 19 mm^3 in vehicle- and glucose-treated rats, respectively. There was a significant, positive linear correlation between T_2-derived infarct volume at 24 h and blood glucose levels 4 h after MCAO in rats that received glucose (R^2=0.43) but not vehicle (R^2=0.15) (Figure 5(b)). Thus, hyperglycaemia increased acute ADC lesion volume and infarct volume 24 h after MCAO.

Perfusion–diffusion mismatch and ADC-derived penumbra

The volume of tissue with perfusion–diffusion mismatch (Figure 6(a)), an estimate of the volume of the ischaemic penumbra, was comparable between groups at each time point post-MCAO (Figure 6(b)). The mean perfusion–diffusion mismatch volumes at 1 h post-MCAO were 103 ± 31 and 117 ± 36 mm^3 in vehicle- and glucose-treated rats, respectively. The volume of perfusion–diffusion mismatch tissue did not change significantly over time in either group as the mismatch volume at 4 h post-MCAO was 108 and 130 mm^3 in vehicle- and glucose-treated rats, respectively. It is important to mention here that although the volume of mismatch tissue measured at each hour after the onset of MCAO does not significantly change between 1 and 4 h in each group, the tissue within the penumbra will inevitably change over time. Some of the tissue with perfusion–diffusion mismatch will become incorporated into the infarct and this is supported by the fact that the ADC lesion increased over time in both vehicle and glucose treatment groups. Also, as collateral blood supply decreases over time (supported by the decrease in CBF observed in the contralateral hemisphere (Figure 3(a)), some of the benign oligaemic tissue will become incorporated into the ischaemic penumbra. Therefore, while the volume of presumed penumbra does not change over time, the tissue compartment defined by the perfusion-diffusion mismatch will have.

Degradation of MAP2 and spectrin levels in ischaemic cortex

The degradation of microtubule-associated protein 2 (MAP2) and spectrin by the calcium-dependent cysteine protease calpain was assessed as a marker of ischaemic brain damage. Calpain cleaves αII-spectrin (280 kDa) producing two spectrin breakdown

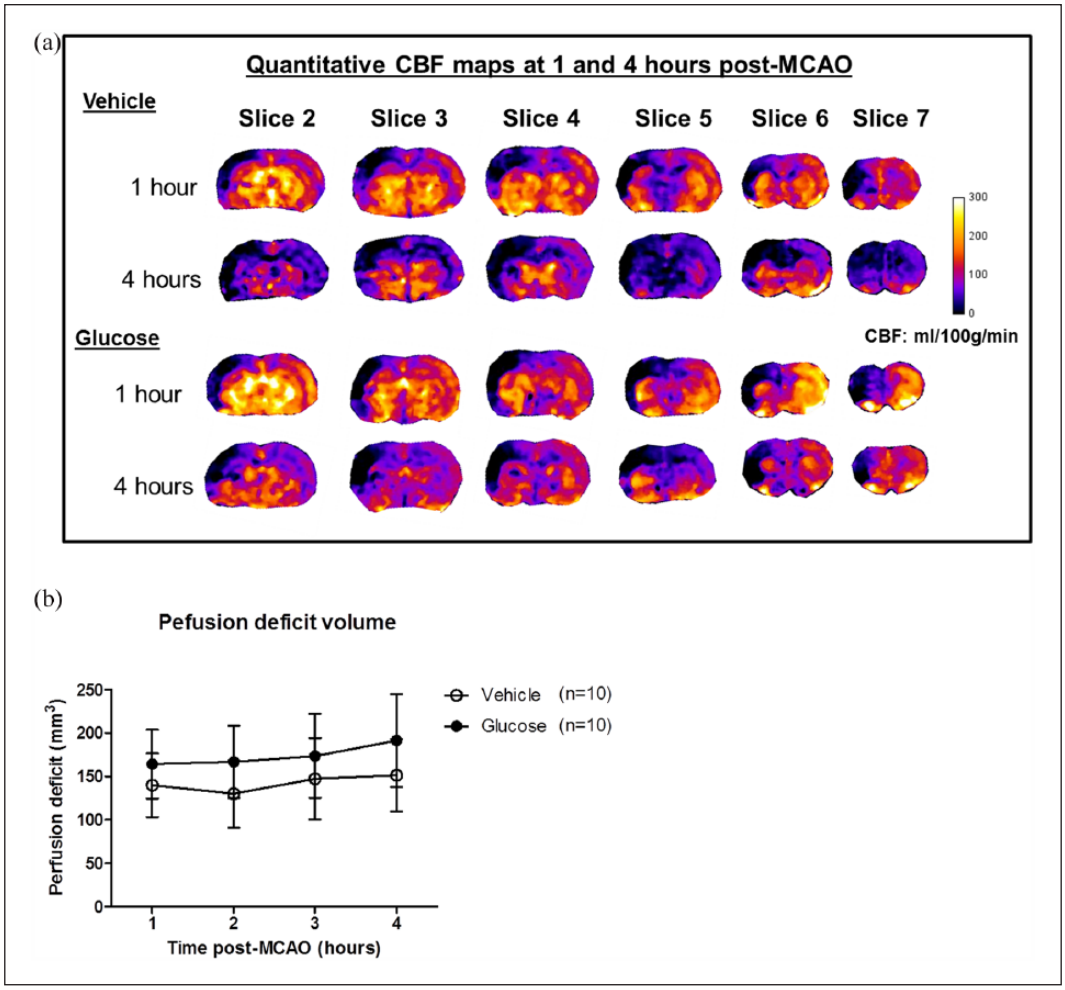

Figure 3. Quantitative CBF maps displaying hypoperfused tissue at 1 and 4 h post-MCAO over six coronal slices (a). The darker regions represent areas with reduced blood flow and these were predominantly in the ipsilateral cortex, as a result of distal MCAO. Temporal evolution of the perfusion deficit 1–4 h after MCAO (b). The perfusion deficit volume was calculated by applying an abnormal perfusion threshold of 30 mL/100 g/min to CBF maps. Data are presented as mean ± standard deviation. Differences between groups are not statistically significant: repeated measures two-way ANOVA with Bonferroni's post-test.

products (SBDPs) at approximately 150 and 145 kDa. In the Western Blot for αII-spectrin, a doublet band representing intact spectrin was observed at 280 kDa in all samples from the vehicle treatment group but was not observed in two rats from the glucose treatment group (G1 and G4) (supplementary Figure 1S). A doublet band representing calpain-mediated SBDPs was observed at 150–155 kDa in all rats. In the two glucose-treated rats, in which a band at 280 kDa was not observed (G1 and G4), an intense band at 150 kDa was observed suggesting a greater extent of calpain-mediated spectrin breakdown in these samples. When the values of the SBDP bands were expressed as a ratio of the β-actin bands, to account for sample loading differences, the relative protein levels of SBDPs were significantly greater in glucose compared to vehicle-treated rats (Figure 1S), suggesting that glucose treatment increased calpain-mediated αII-spectrin breakdown. In the Western blot for MAP2, a band representing MAP2 (high molecular weight isoforms) was observed at approximately 270–280 kDa in most samples (supplementary Figure 2S). The intensity of this MAP2 band varied among samples indicating differing amounts of MAP2 degradation. The intensity was greatest in the control sample (C) where MAP2 proteolysis was expected to be minimal. There was no significant difference in relative MAP2 protein levels (Figure 2S) between glucose and vehicle treatment groups, although relative MAP2 protein levels in glucose-treated rats tended to be lower than vehicle-treated rats.

Discussion

In a model of focal cerebral ischaemia, clinically relevant levels of hyperglycaemia exacerbated the very early evolution of ischaemic brain damage, despite a lack of effect on the volume of perfusion deficit or ischaemia severity, as determined by different methods of CBF measurement. Hyperglycaemia is consistently associated with worse outcomes in both clinical and animal stroke studies. The results reported here support these findings, demonstrating that hyperglycaemia, at levels typically observed in stroke patients, increases acute ischaemic damage and infarct volume in a normotensive rat strain. The rationale for choosing a

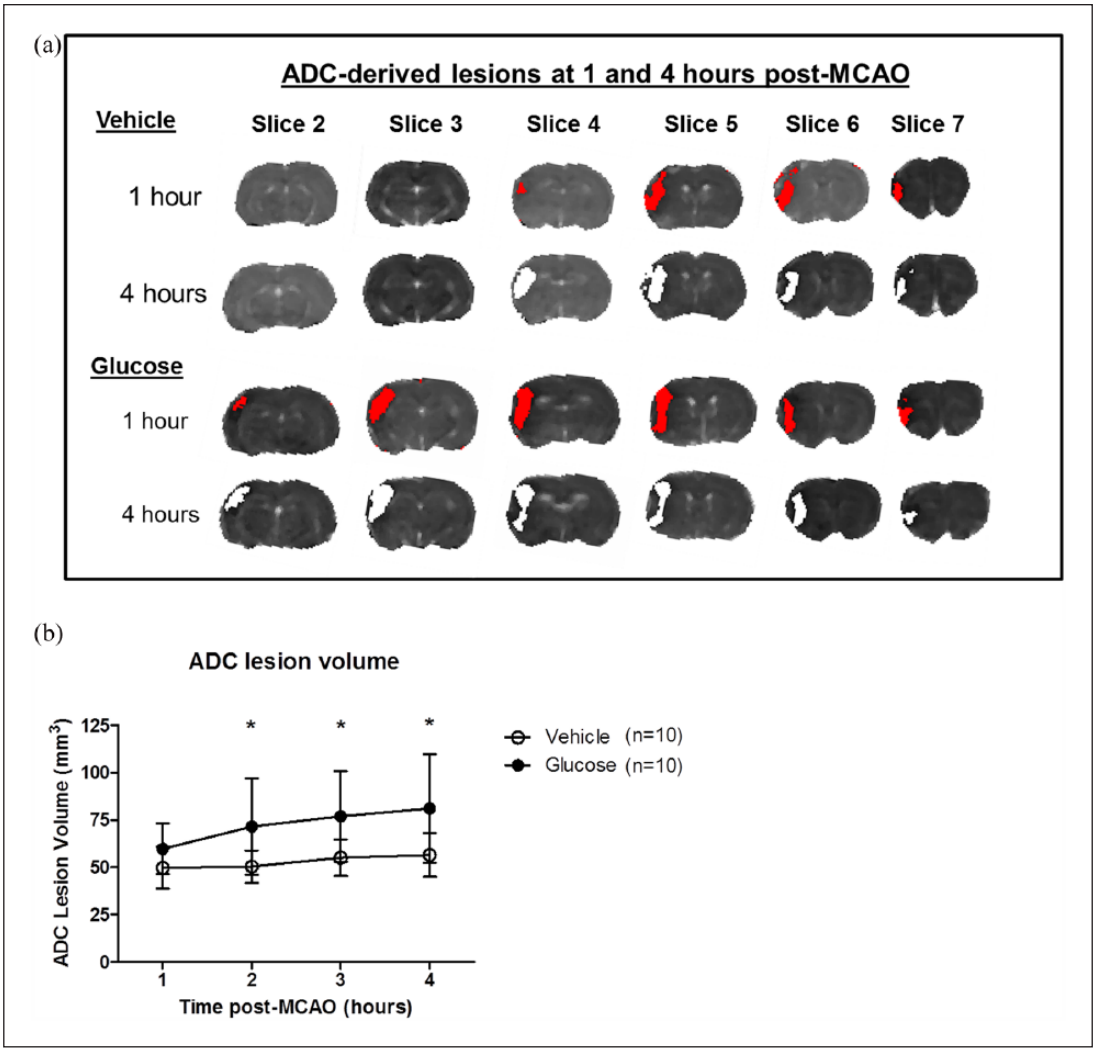

Figure 4. Apparent diffusion coefficient (ADC) lesions at 1 h (white areas) and 4 h (red areas) post-MCAO across the equivalent six coronal slices (a). The images are from the median animal of the vehicle and glucose treatment groups. ADC-derived lesion volume measured 1–4 h after MCAO (b). ADC lesion volume was calculated by applying an abnormal diffusion threshold of 0.53×10^{-3} mm^2/s. Data are presented as mean ± standard deviation. *$P < 0.05$ compared with vehicle rats using a repeated measures two-way ANOVA with Bonferroni's post-test.

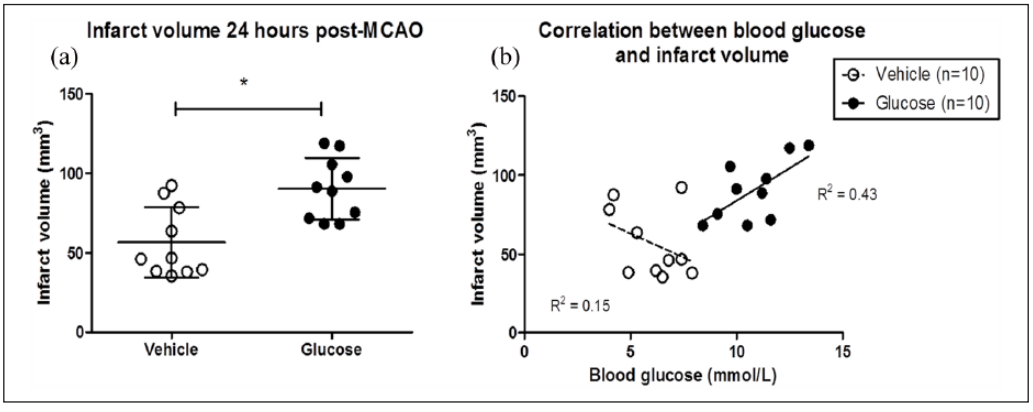

Figure 5. Scatter plot showing the T_2-derived infarct volumes measured 24 h after MCAO in each rat (a). The horizontal line on the scatter plot represents the mean. *$P < 0.05$ compared with vehicle group using a Student's unpaired t-test. A Pearson's correlation was performed between the T_2-derived infarct volume and blood glucose levels measured at 4 h post-MCAO in the vehicle and glucose groups (b). There was a significant, positive correlation between T_2-derived infarct volume and blood glucose levels in rats that received glucose ($R^2 = 0.43$, $P = 0.04$) but not vehicle ($R^2 = 0.15$, $P = 0.3$).

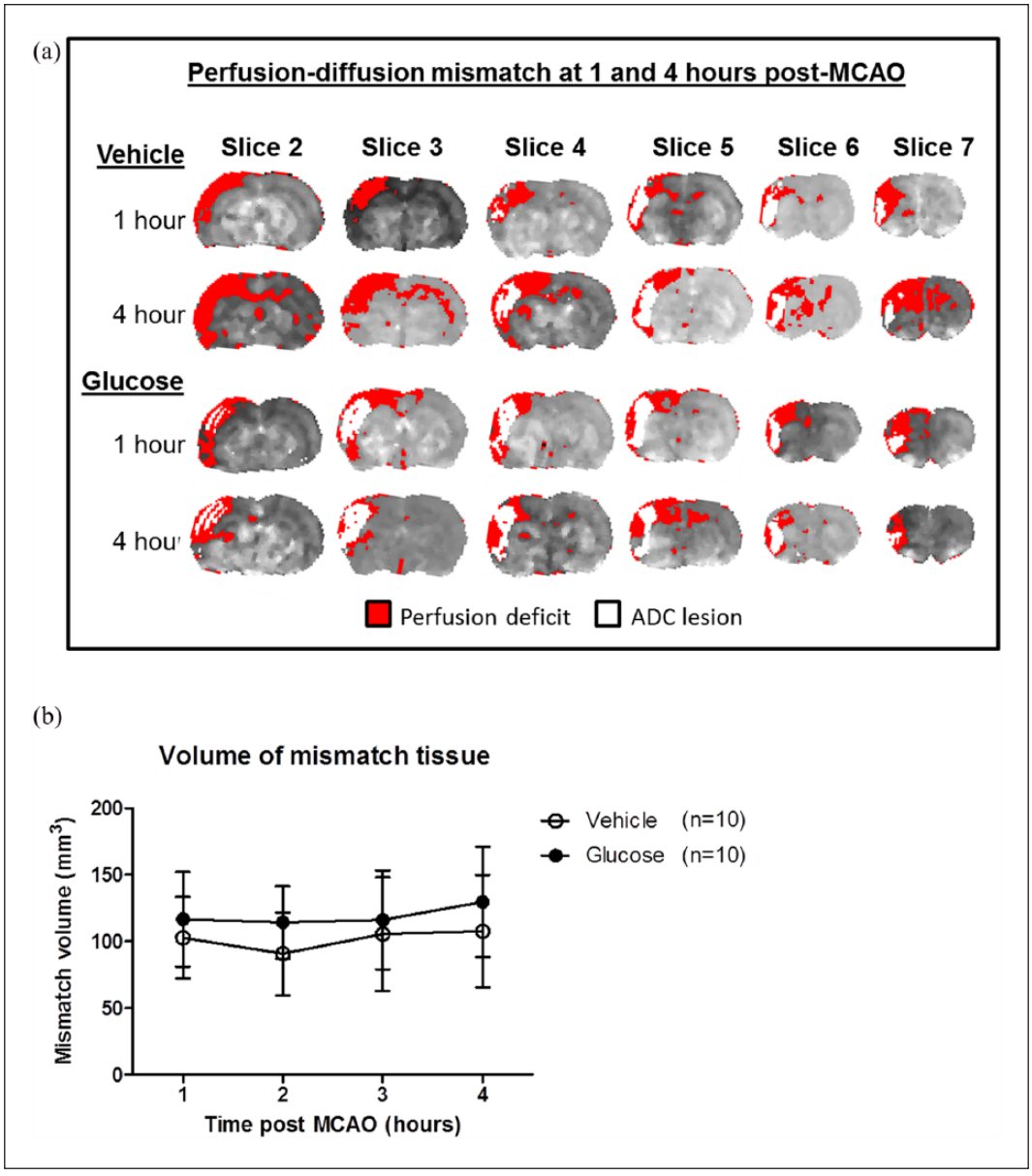

Figure 6. Spatial distributions of perfusion–diffusion mismatch tissue across six coronal slices (caudal to rostral) at 1 and 4 h after MCAO (a). The images displayed are from the median animal of each group. The red region depicts the perfusion deficit defined by applying an absolute threshold of 30 mL/100 g/min. The white region depicts the ADC lesion defined by applying an ADC threshold of 0.53×10^{-3} mm^2/s. On slices where there was a perfusion deficit but no ADC lesion the perfusion deficit area was considered as mismatch tissue. Perfusion–diffusion mismatch volumes 1–4 h post-MCAO (b). There was no statistical difference between vehicle- and glucose-treated groups by repeated measures two-way ANOVA.

normotensive rat strain was based on evidence from clinical and preclinical studies demonstrating that hyperglycaemic patients or animals without co-morbidities (diabetes, metabolic syndrome) had worse outcomes from stroke in comparison to those with additional co-morbidities (Capes et al., 2001; Shimoyama et al., 2014; Tarr et al., 2013). The pathophysiological mechanisms underlying the association between hyperglycaemia and poor outcomes from acute ischaemic stroke are unclear. The data from our present study and from previous studies (Huang et al., 1996; Tarr et al., 2013) show that the detrimental effects of hyperglycaemia occur early, within the first 1–2 h after permanent MCAO leading to significantly larger infarcts. Given this early time-window, and because acute hyperglycaemia has been shown to affect CBF (Duckrow, 1995; Duckrow et al., 1985), we sought to determine whether hyperglycaemia increases ischaemic damage by increasing the volume or severity of the perfusion deficit induced following permanent occlusion of the MCA. We measured cerebral perfusion using two different methods and the results from each demonstrate that hyperglycaemia, at clinically relevant levels, does not induce a significant increase in the severity of hypoperfusion during the first 4 h following MCAO. Previous studies of hyperglycaemia in animal models of stroke have

reported similar findings (Cipolla and Godfrey, 2010; Gisselsson et al., 1999; Marsh et al., 1986; Quast et al., 1997; Venables et al., 1985). For example, Gisselsson and colleagues investigated the influence of hyperglycaemia (20 mmol/L) on tissue damage and CBF in rats during and after transient MCAO. In hyperglycaemic rats, tissue damage after 30 min MCAO was significantly greater compared to normoglycaemic rats but there was no difference in CBF (Gisselsson et al., 1999). In contrast to previous studies, we examined the effects of hyperglycaemia at levels typically observed in patients. In the majority of previous studies, hyperglycaemic animals had blood glucose levels >20 mmol/L, with values exceeding 40 mmol/L in some cases (Marsh et al., 1986). These values far exceed the blood glucose levels classified as hyperglycaemic in patients. For example, in clinical trials investigating insulin treatment for PSH, blood glucose levels in hyperglycaemic patients ranged from ~7 to 10 mmol/L (Gray et al., 2007; Johnston et al., 2009). Physiological blood glucose concentrations are closely regulated and ranged from 4 to 6 mmol/L. Therefore, clinically, only minor increments in blood glucose levels (~1–6 mmol/L) are defined as PSH and have been associated with poorer clinical outcomes. In our animal model, the blood glucose difference between vehicle and glucose-treated rats was ~6 mmol/L, with mean blood glucose values in hyperglycaemic animals (~12 mmol/L) closer to those seen in stroke patients. In one of the few clinical studies to examine perfusion deficits in stroke patients with PSH, mean blood glucose levels in normoglycaemic and hyperglycaemia patients were 5.9 and 9.5 mmol/L, respectively, on admission (Luitse et al., 2013). In the aforementioned study, Luitse and colleagues reported that patients with admission hyperglycaemia did not have larger volumes of hypoperfusion compared to normoglycaemic patients during the acute stage (<24 h) of ischaemic stroke (Luitse et al., 2013). Thus, our results are in agreement with these clinical findings and support the supposition that the detrimental effects of hyperglycaemia in ischaemic stroke are not associated with larger volumes of hypoperfusion.

Although we did not find an effect of hyperglycaemia on cerebral perfusion in our study, hyperglycaemia exacerbated the evolution of ischaemic brain damage, as reflected by larger ADC lesions as early as 2 h after MCAO. This agrees with our previous findings in the Wistar-Kyoto (WKY) and spontaneously hypertensive stroke-prone rat strains where the effects of hyperglycaemia on ADC lesion volume growth were evident as early as 1 h after MCAO (Tarr et al., 2013). One limitation of both studies is that we did not include an isotonic control for glucose-treated group. However, the weight of evidence from clinical studies of stroke patients indicates that naturally occurring hyperglycaemia is associated with poorer outcome than euglycaemia (see above). The pathophysiological mechanisms by which hyperglycaemia increases early ischaemic damage have not been fully elucidated. Possible mechanistic explanations include impaired recanalisation and increased reperfusion injury, increased lactic acidosis, enhancing excitotoxicity and increased oxidative stress and inflammation. Of these many mechanisms, the anaerobic metabolism of glucose through the lactic acid cycle was the first and is the most persistent hypothesis used to explain the relationship between hyperglycaemia and poor outcomes from ischaemic stroke. In the absence of oxygen, glucose is metabolised anaerobically producing lactate as a by-product. Elevated lactate levels can acidify cells and the surrounding environment leading to tissue acidosis. This is potentially damaging and can lead to the production of free radicals and mitochondrial dysfunction (Anderson et al., 1999; Rehncrona et al., 1989), both of which would be detrimental during ischaemia. Both clinical and experimental studies have revealed an association between hyperglycaemia and increased brain lactate levels. Furthermore, elevated lactic acid concentrations have been shown to correlate with worse outcomes (Anderson et al., 1999; LaManna et al., 1992). Although there appears to be strong evidence indicating increased lactate as an important mediator of hyperglycaemia-induced brain damage, the fact that lactate metabolism is important for ATP production during ischaemia (Pellerin and Magistretti, 1994), and that inhibiting lactate production during ischaemia exacerbates, rather than reduces, ischaemic damage (Cassady et al., 2001), suggests that it is not the only contributor.

During the acute 1–2 h following MCAO, when hyperglycaemia had the biggest impact on lesion size, we wanted to determine whether hyperglycaemia had any influence on the volume of penumbra tissue as results from a clinical study demonstrated that larger infarcts in patients with PSH were associated with reduced salvage of penumbra tissue (Parsons et al., 2002). The MRI data produced in our study allowed us to investigate the ischaemic penumbra by measuring the volume of perfusion–diffusion mismatch tissue. We found that hyperglycaemia did not significantly alter the volume of perfusion–diffusion mismatch tissue over the first 4 h after MCAO compared to control. We used a threshold of 30 mL/100 g/min to establish the volume of tissue with a perfusion deficit in our pCASL CBF maps. This may have resulted in an overestimation of the perfusion deficit, as the tissue with a perfusion deficit was not all incorporated into the infarct measured at 24 h. For example, in the group that received glucose, the perfusion deficit at 4 h was 192 mm^3 whereas the ADC lesion volume and T_2-derived infarct volumes were 81 and 90 mm^3, respectively. A potential explanation why most of the perfusion deficit was not incorporated into the final infarct could be the increase in blood pressure that occurs on withdrawal of anaesthesia. Withdrawal of isoflurane, which is known to have a cardio-depressant effect (Schappert et al., 1992), will inevitably lead to a rise in blood pressure as animals regain consciousness. This increase in blood pressure may cause an increase in CBF within the ischaemic hemisphere, reducing the volume of the perfusion deficit and preventing the progression of the hypoperfused at-risk tissue to infarction.

If the adverse effects of hyperglycaemia after stroke are not predominantly mediated at the level of the cerebrovasculature through increased severity of hypoperfusion, the alternative is that the effects take place mainly within brain tissue. In our previous study of hyperglycaemia and MCAO, we reported a small increase in the levels of 4-hydroxynonenal, a marker of oxidative stress, within the infarcts of hyperglycaemic compared to normoglycaemic rats. But this was only detected in normotensive WKY rats, not in fructose-fed, spontaneously hypertensive stroke-prone rats, a model of metabolic syndrome (Tarr et al., 2013). In the current study, infarcted tissue was examined by Western blotting for markers of calcium-dependent calpain activity, breakdown of MAP2 and spectrin (Bartus et al., 1995; Czogalla and Sikorski, 2005; Yan et al., 2012), as a means of indirectly assessing excitotoxic mechanisms which are known to be involved in ischaemic damage to neurons. There was a modest increase in spectrin breakdown in glucose – compared to vehicle-treated

animals, but no difference between groups in the levels of MAP2 in the infarcted tissue (supplementary Figures 1S and 2S). Although not definitive, these observations are consistent with the conclusion that a single predominant mechanism leading to hyperglycaemia-induced exacerbation of neuronal damage is unlikely. However, we only examined tissue that was already infarcted as it was available at the end of the MRI study. Therefore, it would be interesting to examine brain tissue at earlier time points when the damage is evolving and given the complexity of the ischaemic cascade, it may be fruitful to use preparations such as acute in vitro slice preparations for future mechanistic studies.

In conclusion, this study demonstrates the lack of a profound effect of hyperglycaemia on the severity and extent of ischaemia after MCAO in the rat. However, the data reinforce the view that the detrimental effects of hyperglycaemia on brain tissue occur rapidly in the ischaemic brain. A plausible hypothesis may therefore be that hyperglycaemia influences multiple pathophysiological mechanisms simultaneously that combine to exacerbate injury. This could include influences on cerebrovascular function that are too subtle to be detected by the methods we employed to measure CBF. Future clinical trials of glucose lowering therapies are only likely to show benefit if they are initiated early after stroke onset.

Acknowledgements

The authors thank Mr Jim Mullin, Mrs Lindsay Gallagher, Mrs Linda Carberry, Dr Mark McLaughlin and staff at the Wellcome Surgical Institute for technical assistance.

Declaration of conflicting interests

The author(s) declared no potential conflicts of interest with respect to the research, authorship and/or publication of this article.

Funding

This work was supported by a PhD studentship to LA Thow from the Medical Research Council, UK and a grant from the British Pharmacological Society Integrative Pharmacology Fund.

References

Anderson RE, Tan WK, Martin HS, et al. (1999) Effects of glucose and PaO_2 modulation on cortical intracellular acidosis, NADH redox state, and infarction in the ischemic penumbra. *Stroke* 30(1): 160–170.

Bartus RT, Dean RL, Cavanaugh K, et al. (1995) Time-related neuronal changes following middle cerebral artery occlusion: Implications for therapeutic intervention and the role of calpain. *Journal of Cerebral Blood Flow & Metabolism* 15(6): 969–979.

Baskerville TA, McCabe C, Weir CJ, et al. (2012) Noninvasive MRI measurement of CBF: Evaluating an arterial spin labelling sequence with ^{99m}Tc-HMPAO CBF autoradiography in a rat stroke model. *Journal of Cerebral Blood Flow & Metabolism* 32(6): 973–977.

Bevers MB, Vaishnav NH, Pham L, et al. (2016) Hyperglycemia is associated with more severe cytotoxic injury after stroke. *Journal of Cerebral Blood Flow & Metabolism* 37(7): 2577–2583.

Campbell BC and Macrae IM (2015) Translational perspectives on perfusion-diffusion mismatch in ischemic stroke. *International Journal of Stroke* 10(2): 163–162.

Capes SE, Hunt D, Malmberg K, et al. (2001) Stress hyperglycemia and prognosis of stroke in nondiabetic and diabetic patients: A systematic overview. *Stroke* 32(10): 2426–2432.

Cassady CJ, Phillis JW and O'Regan MH (2001) Further studies on the effects of topical lactate on amino acid efflux from the ischemic rat cortex. *Brain Research* 901(1–2): 30–37.

Cipolla MJ and Godfrey JA (2010) Effect of hyperglycemia on brain penetrating arterioles and cerebral blood flow before and after ischemia/reperfusion. *Translational Stroke Research* 1(2): 127–134.

Czogalla A and Sikorski AF (2005) Spectrin and calpain: A 'target' and a 'sniper' in the pathology of neuronal cells. *Cellular and Molecular Life Sciences* 62(17): 1913–1924.

Duckrow RB (1995) Decreased cerebral blood flow during acute hyperglycemia. *Brain Research* 703(1–2): 145–150.

Duckrow RB, Beard DC and Brennan RW (1985) Regional cerebral blood flow decreases during hyperglycemia. *Annals of Neurology* 17(3): 267–272.

Duckrow RB, Beard DC and Brennan RW (1987) Regional cerebral blood flow decreases during chronic and acute hyperglycemia. *Stroke* 18(1): 52–58.

Gerriets T, Stolz E, Walberer M, et al. (2004) Noninvasive quantification of brain edema and the space-occupying effect in rat stroke models using magnetic resonance imaging. *Stroke* 35(2): 566–571.

Gisselsson L, Smith ML and Siesjo BK (1999) Hyperglycemia and focal brain ischemia. *Journal of Cerebral Blood Flow & Metabolism* 19(3): 288–297.

Gray CS, Hildreth AJ, Sandercock PA, et al. (2007) Glucose-potassium-insulin infusions in the management of post-stroke hyperglycaemia: The UK Glucose Insulin in Stroke Trial (GIST-UK). *Lancet Neurology* 6(5): 397–406.

Hoehn-Berlage M, Eis M, Back T, et al. (1995) Changes of relaxation times (T1, T2) and apparent diffusion coefficient after permanent middle cerebral artery occlusion in the rat: Temporal evolution, regional extent, and comparison with histology. *Magnetic Resonance in Medicine* 34(6): 824–834.

Huang J-Y, Li L-T, Wang H, et al. (2014) In vivo two-photon fluorescence microscopy reveals disturbed cerebral capillary blood flow and increased susceptibility to ischemic insults in diabetic mice. *CNS Neuroscience & Therapeutics* 20(9): 816–822.

Huang NC, Wei J and Quast MJ (1996) A comparison of the early development of ischaemic brain damage in normoglycaemic and hyperglycaemic rats using magnetic resonance imaging. *Experimental Brain Research* 109(1): 33–42.

Johnston KC, Hall CE, Kissela BM, et al. (2009) Glucose Regulation in Acute Stroke Patients (GRASP) trial: A randomized pilot trial. *Stroke* 40(12): 3804–3809.

Kawai N, Keep RF, Betz AL, et al. (1998) Hyperglycemia induces progressive changes in the cerebral microvasculature and blood-brain barrier transport during focal cerebral ischemia. *Acta Neurochirurgica Supplementum* 71: 219–221.

LaManna JC, Griffith JK, Cordisco BR, et al. (1992) Intracellular pH in rat brain in vivo and in brain slices. *Canadian Journal of Physiology and Pharmacology* 70(suppl.): S269–277.

Luitse MJ, van Seeters T, Horsch AD, et al. (2013) Admission hyperglycaemia and cerebral perfusion deficits in acute ischaemic stroke. *Cerebrovascular Diseases* 35(2): 163–167.

McCormick M, Hadley D, McLean JR, et al. (2010) Randomized, controlled trial of insulin for acute poststroke hyperglycemia. *Annals of Neurology* 67(5): 570–578.

MacDougall NJ and Muir KW (2011) Hyperglycaemia and infarct size in animal models of middle cerebral artery occlusion: Systematic review and meta-analysis. *Journal of Cerebral Blood Flow & Metabolism* 31(3): 807–818.

Marsh WR, Anderson RE and Sundt TM Jr (1986) Effect of hyperglycemia on brain pH levels in areas of focal incomplete cerebral ischemia in monkeys. *Journal of Neurosurgery* 65(5): 693–696.

Mayhan WG and Patel KP (1995) Acute effects of glucose on reactivity of cerebral microcirculation: Role of activation of protein kinase C. *American Journal of Physiology* 269(4 Pt 2): H1297–1302.

Melamed E (1976) Reactive hyperglycaemia in patients with acute stroke. *Journal of the Neurological Sciences* 29(2–4): 267–275.

Muir KW, McCormick M, Baird T, et al. (2011) Prevalence, predictors and prognosis of post-stroke hyperglycaemia in acute stroke trials: Individual patient data pooled analysis from the Virtual International Stroke Trials Archive (VISTA). *Cerebrovascular Diseases Extra* 1(1): 17–27.

Parsons MW, Barber PA, Desmond PM, et al. (2002) Acute hyperglycemia adversely affects stroke outcome: A magnetic resonance imaging and spectroscopy study. *Annals of Neurology* 52(1): 20–28.

Paxinos GWC (2007) *The Rat Brain in Stereotaxic Coordinates*. London: Elsevier.

Pellerin L and Magistretti PJ (1994) Glutamate uptake into astrocytes stimulates aerobic glycolysis: A mechanism coupling neuronal activity to glucose utilization. *Proceedings of the National Academy of Sciences of the United States of America* 91(22): 10625–10629.

Quast MJ, Wei J, Huang NC, et al. (1997) Perfusion deficit parallels exacerbation of cerebral ischemia/reperfusion injury in hyperglycemic rats. *Journal of Cerebral Blood Flow & Metabolism* 17(5): 553–559.

Rehncrona S, Hauge HN and Siesjo BK (1989) Enhancement of iron-catalyzed free radical formation by acidosis in brain homogenates: Differences in effect by lactic acid and CO_2. *Journal of Cerebral Blood Flow & Metabolism* 9(1): 65–70.

Reid E, Graham D, Lopez-Gonzalez MR, et al. (2012) Penumbra detection using PWI/DWI mismatch MRI in a rat stroke model with and without comorbidity: Comparison of methods. *Journal of Cerebral Blood Flow & Metabolism* 32(9): 1765–1777.

Rosso C, Attal Y, Deltour S, et al. (2011) Hyperglycemia and the fate of apparent diffusion coefficient-defined ischemic penumbra. *AJNR American Journal of Neuroradiology* 32(5): 852–856.

Schappert T, Himmel HM and Ravens U (1992) Differences in cardiodepressant effects of halothane and isoflurane after inotropic stimulation in guinea-pig papillary muscles. *Archives internationales de pharmacodynamie et de thérapie* 320: 43–55.

Shen Q, Meng X, Fisher M, et al. (2003) Pixel-by-pixel spatiotemporal progression of focal ischemia derived using quantitative perfusion and diffusion imaging. *Journal of Cerebral Blood Flow & Metabolism* 23(12): 1479–1488.

Shimoyama T, Kimura K, Uemura J, et al. (2014) Elevated glucose level adversely affects infarct volume growth and neurological deterioration in non-diabetic stroke patients, but not diabetic stroke patients. *European Journal of Neurology* 21(3): 402–410.

Shimoyama T, Kimura K, Uemura J, et al. (2016) Post stroke dysglycemia and acute infarct volume growth: A study using continuous glucose monitoring. *European Journal of Neurology* 76(3–4): 167–174.

Staszewski J, Brodacki B, Kotowicz J, et al. (2011) Intravenous insulin therapy in the maintenance of strict glycemic control in nondiabetic acute stroke patients with mild hyperglycemia. *Journal of Stroke and Cerebrovascular Diseases* 20(2): 150–154.

Swanson RA, Morton MT, Tsao-Wu G, et al. (1990) A semiautomated method for measuring brain infarct volume. *Journal of Cerebral Blood Flow & Metabolism* 10(2): 290–293.

Tamura A, Graham DI, McCulloch J, et al. (1981) Focal cerebral ischaemia in the rat: 1. Description of technique and early neuropathological consequences following middle cerebral artery occlusion. *Journal of Cerebral Blood Flow & Metabolism* 1(1): 53–60.

Tarr D, Graham D, Roy LA, et al. (2013) Hyperglycemia accelerates apparent diffusion coefficient-defined lesion growth after focal cerebral ischemia in rats with and without features of metabolic syndrome. *Journal of Cerebral Blood Flow & Metabolism* 33(10): 1556–1563.

Venables GS, Miller SA, Gibson G, et al. (1985) The effects of hyperglycaemia on changes during reperfusion following focal cerebral ischaemia in the cat. *Journal of Neurology, Neurosurgery, and Psychiatry* 48(7): 663–669.

Wagner KR, Kleinholz M, de Courten-Myers GM, et al. (1992) Hyperglycemic versus normoglycemic stroke: Topography of brain metabolites, intracellular pH, and infarct size. *Journal of Cerebral Blood Flow & Metabolism* 12(2): 213–222.

Wang Z, Luo W, Li P, et al. (2008) Acute hyperglycemia compromises cerebral blood flow following cortical spreading depression in rats monitored by laser speckle imaging. *Journal of Biomedical Optics* 13(6): 064023.

Williams DS, Detre JA, Leigh JS, et al. (1992) Magnetic resonance imaging of perfusion using spin inversion of arterial water. *Proceedings of the National Academy of Sciences of the United States of America* 89(1): 212–216.

Yan X-X, Jeromin A and Jeromin A (2012) Spectrin Breakdown Products (SBDPs) as potential biomarkers for neurodegenerative diseases. *Current Translational Geriatrics and Experimental Gerontology Reports* 1(2): 85–93.